

Thermal characteristics of Cu-based oxygen carriers

Hou-yin Zhao · Yan Cao · Zhi-zhong Kang ·
Yau-bang Wang · Wei-ping Pan

NATAS2011 Conference Special Chapter
© Akadémiai Kiadó, Budapest, Hungary 2011

Abstract Chemical looping combustion (CLC) is a novel combustion technology with the capability for segregation of exhaust products (i.e., carbon dioxide/H₂O or N₂/O₂). The combustion is performed in two interconnected reactors with a solid oxygen carrier circulating between them, transferring oxygen from the air to the fuel. The feasibility of a successful CLC system depends on the selection of an appropriate oxygen carrier. Cu-based oxygen carriers are good oxygen carriers due to high reactivity. However, it faces low melting point, agglomeration problems in fluidized bed. In this study, a circular reduction–oxidation reaction simulated to the cyclic operation of the Cu-based oxygen carrier was conducted on the thermogravimetric analyzer (TG). The thermal behaviors of the potential Cu-based oxygen carrier were investigated by using an X-ray diffraction (XRD), scanning electron microscope (SEM), and surface analyzer. Multiple TG results show that the weight loss was 3.4%, indicating that the loading CuO amount was 17%. Moreover, the weight loss and weight gain was equal during 73 redox cycles, suggesting the good thermal stability of the oxygen carrier. The conversion rate of reduction and oxidation for each redox cycle remained constant even after 73 redox cycles. XRD results show the

new phase formation of CuAl₂O₄ during redox cycles, which promotes the thermal stabilization of the oxygen carrier. The surface area of the oxygen carrier decreased from 105 to 13 m² g⁻¹ after 73 redox cycles and the particle size distribution shifted from 5–15 nm to 15–30 nm, suggesting that the micropores were blocked or collapsed. However, the reactivity of the oxygen carrier didn't decrease. SEM results show that CuO was evenly distributed on the surface of Al₂O₃ after 73 redox cycles. Overall, these results suggested that the Cu-based oxygen carrier was ready for fluidized bed tests.

Keywords Cu-based oxygen carrier · TG · SEM · XRD · Surface area

Introduction

Chemical looping combustion (CLC) is a clean combustion technology with inherent separation of carbon dioxide. CLC involves the use of a metal oxide as an oxygen carrier, which transfers oxygen from the air to the fuel, thus avoiding the direct contact between fuel and air [1]. The system is made of two interconnect reactors, air and fuel reactors [2, 3]. In the air reactor, the oxygen carrier is first oxidized by the air, thus extracting oxygen from the air. The exit gas leaving the air reactor contains N₂ and unreacted O₂ [2]. After being transferred to the fuel reactor, the oxygen carrier is reduced, thus oxidizing the fuel. Hence, the reduced metal oxide is ready to be transferred to the to the air reactor and recycled. The exit gas from the fuel reactor contains CO₂ and H₂O. If the water was condensed, concentrated CO₂ streams can be obtained with little energy lost for component separation [2, 3]. An efficient oxygen carrier is one of the essential parameters to successfully operate the CLC system, which

H. Zhao · Y. Cao · W. Pan (✉)
Institute for Combustion Science & Environmental Technology,
Western Kentucky University, Bowling Green, KY 42101, USA
e-mail: wei-ping.pan@wku.edu

Z. Kang
School of Energy, Power and Mechanical Engineering,
North China Electric Power University, Changping District,
Beijing 102206, China

Y. Wang
Mingchi University, 84 Gungjuan Rd, Taipei 24301,
Taiwan, ROC

needs high reactivity and oxygen-transfer capacity and favorable thermodynamics [2–8]. Many different metal-based oxides have been tested in the literature as potential candidates for CLC systems, for example, nickel (Ni) [3–6], copper (Cu) [2–4, 7–10], iron (Fe) [3–6], cobalt (Co) [3, 11, 12], and manganese (Mn) [3, 4]. Among these oxygen carriers, iron and copper oxygen carriers are good candidates for CLC system because of low expense, environmental friendliness, and good oxygen capacities [2–4, 8, 9]. Compared with Cu-based oxygen carriers, the reactivity of Fe-based oxygen carriers was lower [3, 9], so Cu-based oxygen carriers were more widely used. However, the Cu-based oxygen carriers face the agglomeration, accumulative thermal sintering problems during cyclic operations [2, 4]. Therefore, solving these issues is an important step for Cu-based oxygen carriers. In this study, a circular redox of the Cu-based oxygen carrier was conducted in a TG and the thermal behaviors of the oxygen carrier were characterized by using an XRD, SEM, and surface analyzer.

Experimental

Oxygen carrier preparation

The substrate used in this experiment was commercial γ -Al₂O₃ (Puralox NWA-155 Sasol Germany GmbH) with particle size of 100–300 μm , density of 1.3 g cm⁻³, and a porosity of 55.4%. Copper nitrate from Acros (USA) was chosen as the precursor. The oxygen carrier was prepared using a dry impregnation method. In this process, a water-based solution of saturated Cu(NO₃)₂, a small amount of thermal durability enhanced reagents and dispersants were mixed for 12 h. After mixing, the solution was applied to the substrate γ -Al₂O₃ until fully wetted. Then the ethanol was continuously applied to the oxygen carrier for roughly 30 min and dried in the oven at 150 °C for 2 h. After removing from the oven, the carrier was treated again with the saturated Cu(NO₃)₂ solution followed by the ethanol treatment and 2 more hours at 150 °C. Subsequently, the carrier was calcinated in the oven at 500 °C for 5 h. XRD results show that at this point, the oxygen carrier was a black mixture of CuO and Al₂O₃.

Multiple TG analysis

The multiple TG measurement was obtained using a TA Instruments 2950 TG. A 20 mg sample was placed in a platinum pan and heated to 800 °C in nitrogen flow, and then exposed in a cyclic manner to a reducing gas of 10% H₂ for the reduction period and to an oxidizing gas of air for the oxidation period. The temperature was kept at 800 °C. The reduction and oxidation periods were

50–300 s, respectively. N₂ was introduced for 600 s between periods to avoid mixing between H₂ and oxygen. The total flow of the gas into the furnace was 100 mL min⁻¹ and a 10% portion of the total gas flow, i.e., 10 mL min⁻¹ purge N₂ was introduced from the head of TG to keep the balance parts from any corrosive gas.

The conversion rate for reduction and oxidation was calculated according to Eqs. 1 and 2.

$$X_{\text{ox}} = \frac{(m - m_{\text{red}})}{(m_{\text{ox}} - m_{\text{red}})} \quad (1)$$

$$X_{\text{red}} = 1 - X_{\text{ox}} \quad (2)$$

where m is the actual mass of the oxygen carrier, m_{ox} is the maximum amount of the oxygen carrier fully oxidized and m_{red} is the minimum amount of the oxygen carrier fully reduced.

Pore structure analysis

The surface area of the carrier was characterized by a Micromeritics ASAP 2020. The apparent surface area of the carriers was evaluated from the N₂ adsorption isotherms by applying the BET equation in the relative pressure range of 0.05–0.35. The mesopore size was determined using BJH method and the pore size distribution was determined by DFT method.

XRD analysis

The identification of the crystalline phases of the carriers was carried out using a SCINTAG X'TRA AA85516 (ThermoARL) X-ray diffractometer equipped with a Peltier cooled Si solid detector. Monochromatized Cu K α 1 (0.154 nm) was used as the radiation. Diffraction patterns were collected at 45 kV–40 mA, at 0.01° step and count time of 0.500 s over a range of 5.00°–90.00° (2θ), at a step scan rate of 1.20° min⁻¹.

SEM observation

The morphology characterization of the carrier was determined by a JEOL JSM 5400-LV scanning electron microscope. The copper distribution in the cross section was also determined by embedding the particle in resin, polishing to reveal cross section, and then analyzing by SEM.

Results and discussion

TG results

In the TG experiments, the tests were performed at 800 °C because at higher temperatures CuO will decomposed to

Cu_2O in N_2 atmosphere. The results show the weight loss of the oxygen carrier was 3.4%, indicating the loading CuO amount was 17% (Fig. 1). Moreover, the weight loss and the weight gain during reduction and oxidation periods were equal even after 73 redox tests, demonstrating that the carrier has good thermal stability. However, for the pure CuO and Cu_2O , the weight loss and weight gain decreased dramatically after 3 redox cycles (Fig. 2), which means the worse thermal stability. As a result, they are not suitable for oxygen carriers, which is similar to the results of others [2, 13]. The different thermal stability between the oxygen carrier and CuO and Cu_2O was due to the new formation of the CuAl_2O_4 during oxidation. XRD results showed the new formation of CuAl_2O_4 spinel during the redox cycles. Figure 3 shows that the fresh oxygen carrier was composed

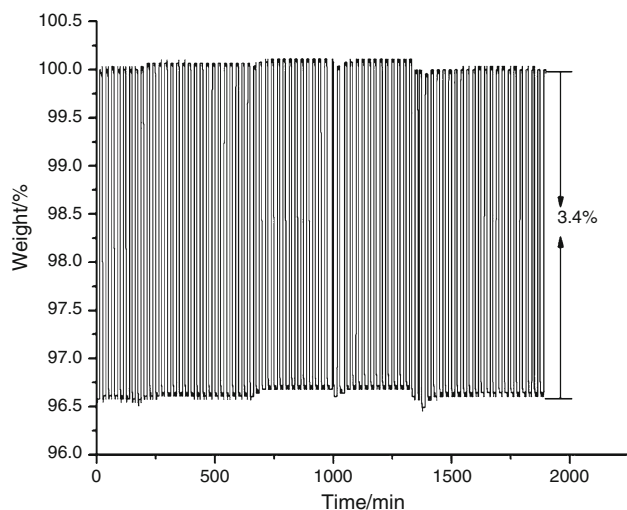


Fig. 1 TG curve for the carrier vs time for 73 redox cycle tests

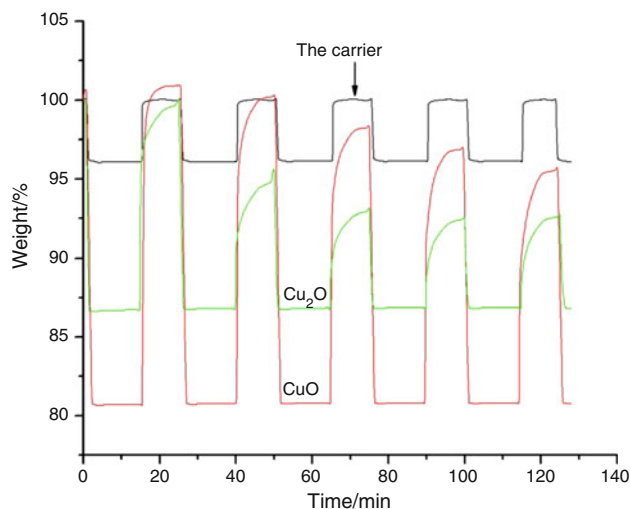


Fig. 2 Overlay of TG curves of CuO , Cu_2O , and the carrier

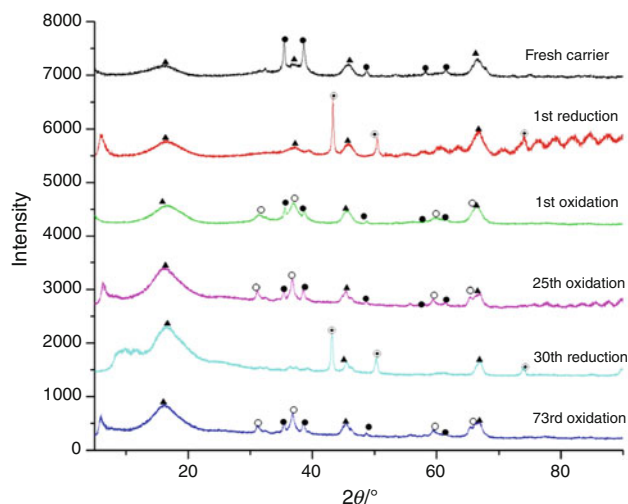


Fig. 3 XRD spectrum for the oxygen carriers (filled circle CuO , filled triangle Al_2O_3 , open circle CuAl_2O_4 , encircled dot Cu)

of CuO and Al_2O_3 . After the first reduction, it was reduced to Cu while after first oxidation, it was oxidized to CuAl_2O_4 , CuO , and Al_2O_3 , where CuAl_2O_4 formed (Fig. 3). In the oxidation condition, after 25 and 73 redox cycles, the composition still was CuAl_2O_4 , CuO , and Al_2O_3 . Researchers found that the addition of a binder increased the oxidation rate and concluded that the binder plays dual roles: one as an oxygen-permeable material and two as a material to enhance the mechanical strength of the particle for cyclic use and against abrasion [2]. So in this experiment, the new formation of CuAl_2O_4 spinel played this important role, which promoted the stabilization of the oxygen carrier. In the reduction condition, the composition was mainly Cu and Al_2O_3 , indicating that the oxygen carrier was completely reduced.

The reduction and oxidation conversion rate of the oxygen carrier was shown in Fig. 4. It can be seen that the reduction and oxidation was fully converted in 45 s, indicating high reactivity, consistent with other researchers [14, 15]. After 73 redox cycles, the conversion rate of reduction and oxidation was still similar, implying that the carrier's reactivity was not affected by the number of cycles in use.

Using SEM-EDX and surface area analyzer, the structure and particle distribution of the oxygen carrier was studied. SEM results showed that CuO was evenly distributed on the surface of the Al_2O_3 for the fresh oxygen carrier (bright point was copper and oxygen, black was aluminum and oxygen) (Fig. 5a) and after 73 redox cycles the CuO was still evenly distributed on the surface and there was no agglomeration (Fig. 5b). The particle size was less than $5\ \mu\text{m}$. The cross section of the SEM results indicated that most of the copper oxide was distributed on

Fig. 4 Conversion rate for the oxygen carrier during redox cycles. **a** Reduction. **b** Oxidation

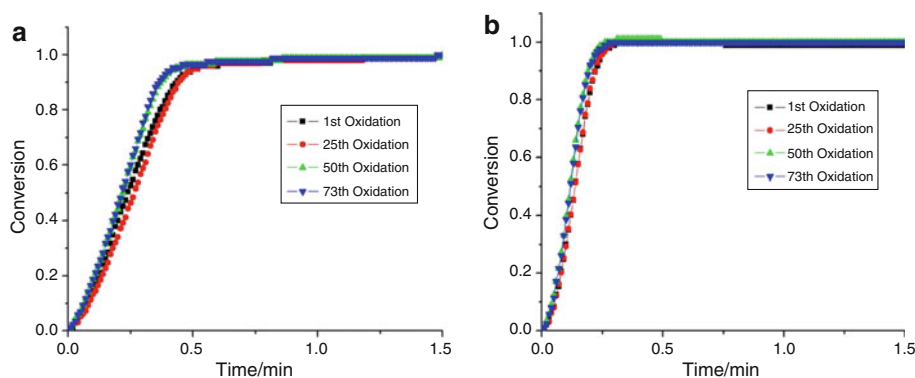


Fig. 5 SEM image for the oxygen carrier. Surface of particle (**a** fresh carrier, **b**: the carrier after 73 redox cycle tests) and cross section (**c** fresh carrier, **d** the carrier after 73 redox cycle tests)

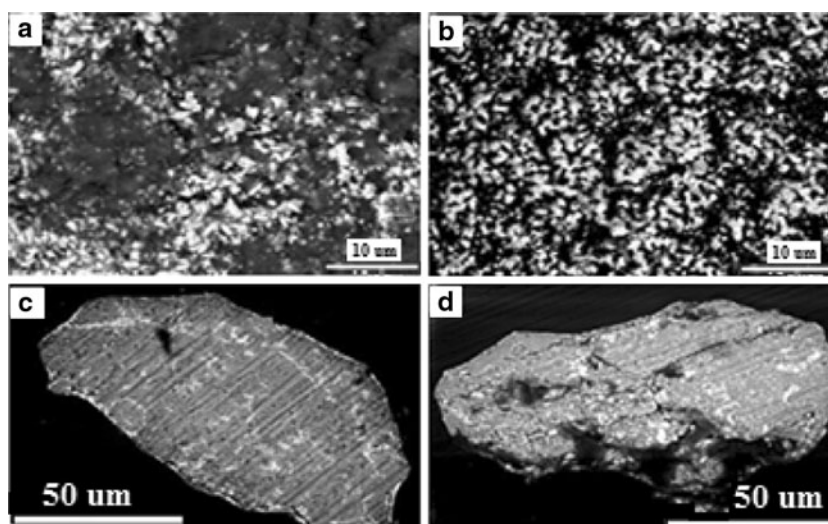


Table 1 Surface area of the oxygen carriers

Sample ID	Surface area/m ² /g	BJH Pore size/nm
Fresh carrier	105	11
Carrier after 25 cycle tests	20	18
Carrier after 73 cycle tests	13	18

the outer layer of the Al₂O₃ for the fresh oxygen carrier (Fig. 5c) and after 73 redox cycles, the thickness of the outlayer decreased and some copper oxide went into the center through the hole or the crack of the Al₂O₃ (Fig. 5d), which may be caused by chemical reaction or thermal shock [16]. Table 1 shows that with increasing redox cycles, the surface area of the oxygen carrier decreased. The surface area of the fresh oxygen carrier was 105 m² g⁻¹, and then decreased to 20 and 13 m² g⁻¹ after 25 and 76 cycle tests, respectively. The pore-size distribution of the oxygen carriers showed that the pore size of the oxygen carrier shifted from 5–15 nm to 15–30 nm after redox cycles, implying that some pores may be blocked or collapsed after cyclic tests (Fig. 6). It can also be seen that

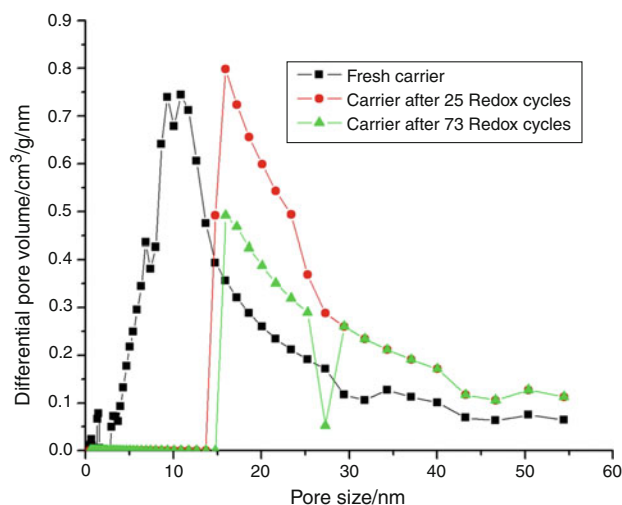


Fig. 6 Pore-size distribution of the carriers

the mesopores (BJH pore size) increased from 11 to 18 nm, indicating the collapse of the micropores. However, the previous TG results (Fig. 1) show that the reactivity of the oxygen carrier didn't decrease.

Conclusions

Chemical looping combustion is a promising technology, where the oxygen carrier plays an important role. The Cu-based oxygen carrier has been paid more attention because of high reactivity. However, it faces the agglomeration problems. A circular reduction and oxidation experiment of the Cu-based oxygen carrier was conducted in the TG and the thermal characterization was investigated by using an XRD, SEM, and surface analyzer. The multiple TG results show that after 73 redox cycles, the thermal stability of the oxygen carrier was still good. Moreover, the conversion rate of reduction and oxidation at each redox cycle test remained constant. XRD results demonstrate the new phase formation of CuAl_2O_4 spinel, which was responsible for the thermal stabilization of the oxygen carrier. SEM results illustrate that CuO was evenly distributed on the surface of Al_2O_3 and there was no agglomeration on the surface. The surface area of the carrier decreased from 105 to $13 \text{ m}^2 \text{ g}^{-1}$ after 73 redox cycles and the particle-size distribution shifted from $5\text{--}15 \text{ nm}$ to $15\text{--}30 \text{ nm}$, suggesting that the micropores collapsed. However, the reactivity of the oxygen carrier didn't change. In summary, the Cu-based oxygen carrier has high thermal stability capacities, which is feasible for CLC systems.

Acknowledgements We gratefully acknowledge financial supports through projects by the United State Department of Energy (DE-FC26-FE0001808).

References

1. Mattisson T, Adanez J, Proell T, Kuusik R, Beal C, Assink J, Snijkers F, Lyngfelt A. Chemical-looping combustion CO_2 ready gas power. *Energy Procedia*. 2009;1:1557–64.
2. De Diego L, Garcia-Labiano F, Adanez J, Gayan P, Abad A, Corbella B, Palacios JM. Development of Cu-based oxygen carriers for chemical-looping combustion. *Fuel*. 2004;83:1749–57.
3. Siriwardane R, Tian HJ, Richard G, Simonyi T, Poston J. Chemical-looping combustion of coal with metal oxide oxygen carriers. *Energy Fuels*. 2009;23:3885–92.
4. Cho P, Mattisson T, Lyngfelt A. Comparison of iron-, nickel, copper- and manganese-based oxygen carriers for chemical-looping combustion. *Fuel*. 2004;83:1215–25.
5. Jerndal E, Mattisson T, Lyngfelt A. Investigation of different NiO/ NiAl_2O_4 particles as oxygen carriers for chemical-looping combustion. *Energy Fuels*. 2009;23:665–76.
6. Wolf J, Anheden M, Yan JY. Comparison of nickel- and iron-based oxygen carriers in chemical looping combustion for CO_2 capture in power generation. *Fuel*. 2005;84:993–1006.
7. Cao Y, Pan WP. Investigation of chemical looping combustion by solid fuels. 1. Process analysis. *Energy Fuels*. 2006;20:1836–44.
8. Tian HJ, Chaudhari K, Simonyi T, Poston J, Liu TF, Sanders T, Veser G, Siriwardane R. Chemical-looping combustion of coal derived synthesis gas over copper oxide oxygen carriers. *Energy Fuels*. 2008;22:3744–55.
9. Garcia-Labiano F, Diego LF, Adanez J, Abad A, Gayan P. Chem. Effect of pressure on the behavior of copper-, iron-, and nickel-based oxygen carriers for chemical-looping combustion. *Eng Sci*. 2005;60:851–62.
10. Moran-Pineda M, Castillo S, Asomoza M, Gomez R. Copper oxide on $\text{Cu}/\text{Al}_2\text{O}_3\text{-TiO}_2$ catalysts TG, FTIR-CO absorption and catalytic activity in the NO reduction by CO. *J Therm Anal Cal*. 2003;73:341–6.
11. Jin HG, Ishida M. A new type of coal gas fueled chemical-looping combustion. *Fuel*. 2004;83:2011–7.
12. Jin HG, Okamoto T, Ishida M. Development of a novel chemical-looping combustion: synthesis of looping material with a double metal oxide of CoO-NiO. *Energy Fuels*. 1998;12(6):1272–7.
13. Ishida M, Jin HG. A novel chemical-looping combustor without NO_x formation. *Ind Eng Chem Res*. 1996;35:2469–72.
14. Degif LF, Gayan P, Garcia-labiano F, Celaya J, Abad A, Adanez J. Impregnated $\text{CuO}/\text{Al}_2\text{O}_3$ oxygen carriers for chemical-looping combustion: avoiding fluidized bed agglomeration. *Energy Fuels*. 2005;19:1850–6.
15. Zafar Q, Abad A, Mattisson T, Gever B. Reaction kinetics of freeze-granulated NiO/ MgAl_2O_4 oxygen carrier particles for chemical-looping combustion. *Energy Fuels*. 2007;21:610–8.
16. Zhao HB, Liu LM, Xu D, Zheng CG, Liu GJ, Jiang LL. NiO/ NiAl_2O_4 oxygen carriers prepared by sol-gel for chemical-looping combustion fueled by gas. *J Fuel Chem Tech*. 2008;36:261–6.